

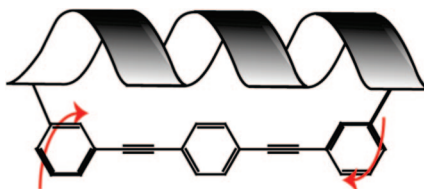
Chirally Twisted Oligo(phenyleneethynylene) by Cyclization with α -Helical Peptide

Hidenori Nakayama and Shunsaku Kimura*

Graduate School of Engineering, Kyoto University, Kyoto-Daigaku-Katsura, Nishikyo-ku, Kyoto 615-8510, Japan

shun@scl.kyoto-u.ac.jp

Received February 11, 2009



A novel cyclic conjugate of a helical decapeptide and oligo(phenyleneethynylene) (OPE), **C-OPE10**, was synthesized. The conformation and the optical properties of the cyclic conjugate were studied by circular dichroism (CD), absorption, and emission spectroscopies. In the cyclic conjugate, the rotational motion around the molecular axis of the OPE moiety was hindered to take a chirally twisted conformation, which is a distorted form from the coplanar conjugated structure, as revealed by observation of an induced negative Cotton effect of the OPE moiety. Molecular simulation using time dependant-density functional theory indicated a right-handed twist conformation of the OPE moiety for the negative Cotton effect. This conjugate therefore provides a new way to obtain a π -conjugated compound having main-chain chirality. The optical properties of the OPE moiety taking the twist conformation in the cyclic conjugate are also discussed in depth.

Introduction

Poly- and oligo(phenyleneethynylene)s (PPE/OPEs) are highly π -conjugated compounds with rigid linear backbone,^{1–5} which are currently attracting great interest in electronic and optical engineering fields. Because one of the emerging applications of the π -conjugated compounds is opto-electronics materials, the fluorescence and the electron transport properties have been studied extensively both from experimental^{6–14} and theoretical^{15–18} aspects. Further, PPEs/OPEs become highly fluorescent

when quenching due to molecular stacking is avoided,^{19–21} which are also useful for application to high-sensitive chemical sensors.^{22–30}

- (1) Bunz, U. H. F. *Chem. Rev.* **2000**, *100* (4), 1605–1644.
- (2) Tour, J. M. *Acc. Chem. Res.* **2000**, *33* (11), 791–804.
- (3) Tour, J. M.; Rawlett, A. M.; Kozaki, M.; Yao, Y.; Jagessar, R. C.; Dirk, S. M.; Price, D. W.; Reed, M. A.; Zhou, C.-W.; Chen, J.; Wang, W.; Campbell, I. *Chem.—Eur. J.* **2001**, *7* (23), 5118–5134.
- (4) Hwang, J.-J.; Tour, J. M. *Tetrahedron* **2002**, *58* (52), 10387–10405.
- (5) Price, D. W.; Dirk, S. M.; Maya, F.; Tour, J. M. *Tetrahedron* **2003**, *59* (14), 2497–2518.
- (6) Dhirani, A.; Lin, P. H.; Guyot-Sionnest, P.; Zehner, R. W.; Sita, L. R. *J. Chem. Phys.* **1997**, *106* (12), 5249–5253.
- (7) Sachs, S. B.; Dudek, S. P.; Hsung, R. P.; Sita, L. R.; Smalley, J. F.; Newton, M. D.; Feldberg, S. W.; Chidsey, C. E. D. *J. Am. Chem. Soc.* **1997**, *119* (43), 10563–10564.
- (8) Bumm, L.; Arnold, J.; Cygan, M.; Dunbar, T.; Burgin, T.; Jones, L.; Allara, D.; Tour, J.; Weiss, P. *Science* **1996**, *271* (5256), 1705–1707.
- (9) Zangmeister, C. D.; Robey, S. W.; vanZee, R. D.; Yao, Y.; Tour, J. M. *J. Phys. Chem. B* **2004**, *108* (41), 16187–16193.
- (10) Selzer, Y.; Cai, L.; Cabassi, M. A.; Yao, Y.; Tour, J. M.; Mayer, T. S.;

- Allara, D. L. *Nano Lett.* **2005**, *5* (1), 61–65.
- (11) Cygan, M. T.; Dunbar, T. D.; Arnold, J. J.; Bumm, L. A.; Shedlock, N. F.; Burgin, T. P.; Jones, L.; Allara, D. L.; Tour, J. M.; Weiss, P. S. *J. Am. Chem. Soc.* **1998**, *120* (12), 2721–2732.
- (12) Moore, A. M.; Dameron, A. A.; Mantooh, B. A.; Smith, R. K.; Fuchs, D. J.; Ciszek, J. W.; Maya, F.; Yao, Y.; Tour, J. M.; Weiss, P. S. *J. Am. Chem. Soc.* **2006**, *128* (6), 1959–1967.
- (13) Moore, A. M.; Mantooh, B. A.; Donhauser, Z. J.; Yao, Y.; Tour, J. M.; Weiss, P. S. *J. Am. Chem. Soc.* **2007**, *129* (34), 10352–10353.
- (14) Beebe, J. M.; Kim, B.; Frisbie, C. D.; Kushmerick, J. G. *ACS Nano* **2008**, *2* (5), 827–832.
- (15) Yin, X.; Li, Y.; Zhang, Y.; Li, P.; Zhao, J. *Chem. Phys. Lett.* **2006**, *422* (1–3), 111–116.
- (16) Segal, D.; Nitzan, A.; Davis, W. B.; Wasielewski, M. R.; Ratner, M. A. *J. Phys. Chem. B* **2000**, *104* (16), 3817–3829.
- (17) Kushmerick, J. G.; Holt, D. B.; Yang, J. C.; Naciri, J.; Moore, M. H.; Shashidhar, R. *Phys. Rev. Lett.* **2002**, *89* (8), 086802–086802.
- (18) Seminario, J. M.; Zacarias, A. G.; Tour, J. M. *J. Am. Chem. Soc.* **1998**, *120* (16), 3970–3974.
- (19) Halkyard, C. E.; Rampey, M. E.; Kloppenburg, L.; Studer-Martinez, S. L.; Bunz, U. H. F. *Macromolecules* **1998**, *31* (25), 8655–8659.
- (20) Li, H.; Powell, D. R.; Hayashi, R. K.; West, R. *Macromolecules* **1998**, *31* (1), 52–58.
- (21) Remmers, M.; Schulze, M.; Wegner, G. *Macromol. Rapid Commun.* **1996**, *17* (4), 239–252.

Fundamental spectroscopic properties of PPE/OPEs have been studied intensively. One of the interesting features in these compounds is an unusual strong asymmetry between absorbance and emission spectra.^{31–35} To interpret this phenomenon several theoretical models have been proposed. Liu et al.³⁶ have successfully reproduced absorption spectra of PPE/OPEs with *ab initio* calculation using the quadratic coupling model.^{37,38} Another characteristic feature is appearance of a sharp bathochromic band in absorption spectra in poor solvents or solid state.^{19,26,39,40} Kim et al. have explained the phenomenon in terms of the conformation of PPE confined in a Langmuir film.⁴⁰ They clearly showed that cofacial π -aggregation was the reason for the sharp band. Masuo et al. encapsulated a PPE rigid chain within dendrimers and found that no bathochromic band was observed even in poor solvating environment or in solid state for the PPE.²⁶

The spectroscopic spectra of PPE/OPEs are strongly dependent on molecular conformation. The rotational barrier of adjacent phenyl rings around the acetylene linkage is known to be less than 1 kcal/mol.^{18,41} The rotational barrier is therefore comparative to $k_B T$ in a solution at room temperature, resulting in near-to-free rotation of the phenyl rings. Since the π -conjugation state of PPE/OPEs is strongly coupled to the dihedral angle of adjacent phenyl rings, spectroscopic properties of PPE/OPEs are tunable by regulating the phenyl ring rotation. Indeed, several efforts have been made to promote the planar conformation of PPE/OPEs.^{42–45} Hu et al. have recently succeeded in inducing the planar conformation of the OPE using intramolecular

hydrogen bond formation.⁴⁵ They showed that the maximum absorption wavelength of the planar OPE was 20–40 nm longer than nonplanar ones. Reversely, if a PPE/OPE is fixed in a twisted conformation, its absorption should show a hypsochromic shift as shown by Brizius et al. who have studied on twisted diphenylacetylenes.⁴⁶ Yang et al. have also reached to the same conclusion from the experiment using pentiptycene-modified OPEs.⁴⁷

In the present work, we tried to regulate rotation of phenyl rings by clipping the two points of OPE with a helical peptide to induce a chirally twisted conformation in the OPE. The key point of using the helical peptide as a bridge for the two terminals of the OPE is to induce main-chain chirality with help of the chiral helicity of the peptide. We synthesized a novel OPE-peptide cyclic conjugate **C-OPE10** as well as a linear conjugate **L-OPE10** as a reference compound (Figure 1). OPE having two carboxyl groups was bridged by a helical decapeptide composed of alternating alanine (Ala) and α -aminoisobutylic acid (Aib). Aib rich oligopeptides are known to take a 3_{10} - or an α -helical structure.⁴⁸ The molecular length of a helical decamer is estimated to be 1.5–2 nm, which is close to that of OPE (1.7 nm). The helical peptide should be effective not only for restriction of the rotational motion in OPE but also for induction of a chiral twist on it. The conformation of the peptide decamer and the OPE moiety were studied by circular dichroism (CD) spectroscopy, and the electronic structures of the OPE moiety were discussed based on absorption and emission spectroscopies. For detailed discussion on CD measurements, *ab initio* calculations were performed using time dependent (TD)-density functional theory (DFT).

Results and Discussion

Conformation of Peptide. To investigate the conformation of the peptide moieties of **L-OPE10** and **C-OPE10**, CD spectra were measured in methanol at room temperature (Figure 2a). The spectrum of **L-OPE10** showed a weak positive Cotton effect around 220 nm, suggesting that two moieties of the peptide pentamers in **L-OPE10** take a disordered conformation,⁴⁹ although some pentamers consisted of Ala and Aib residues are known to take a 3_{10} - or an α -helical structure.⁵⁰ On the other hand, **C-OPE10** showed clearly a double-minimum pattern (peaks at 208 and 222 nm), which is characteristic of an α -helical structure.^{49,51} Otsuda et al. have investigated on the critical length for transition from a 3_{10} - to an α -helix of Boc-(Ala-Aib)_n-OMe to be eight residues on the basis of X-ray analysis of the crystalline structures.⁴⁸ The present observation for the peptide decamer in **C-OPE10** is in agreement with the previous finding.

Although the CD spectrum of **C-OPE10** showed the clear pattern of α -helix, the structure was not so stable. The helix content was determined as 23% and decreased further upon raising temperature from 10 to 50 °C (Figure 2b). These facts

- (22) Zhou, Q.; Swager, T. M. *J. Am. Chem. Soc.* **1995**, *117* (50), 12593–12602.
 (23) Zhou, Q.; Swager, T. M. *J. Am. Chem. Soc.* **1995**, *117* (26), 7017–7018.
 (24) Yang, J. S.; Swager, T. M. *J. Am. Chem. Soc.* **1998**, *120* (46), 11864–11873.
 (25) Yang, J. S.; Swager, T. M. *J. Am. Chem. Soc.* **1998**, *120* (21), 5321–5322.
 (26) Masuo, S.; Yoshikawa, H.; Asahi, T.; Masuhara, H.; Sato, T.; Jiang, D. L.; Aida, T. *J. Phys. Chem. B* **2003**, *107* (11), 2471–2479.
 (27) Sato, T.; Jiang, D. L.; Aida, T. *J. Am. Chem. Soc.* **1999**, *121* (45), 10658–10659.
 (28) Ogoshi, T.; Takashima, Y.; Yamaguchi, H.; Harada, A. *Chem. Commun.* **2006**, (35), 3702–3704.
 (29) McQuade, D. T.; Pullen, A. E.; Swager, T. M. *Chem. Rev.* **2000**, *100* (7), 2537–2574.
 (30) Satrijo, A.; Swager, T. M. *J. Am. Chem. Soc.* **2007**, *129* (51), 16020–16028.
 (31) Cornil, J.; Beljonne, D.; Heller, C. M.; Campbell, I. H.; Laurich, B. K.; Smith, D. L.; Bradley, D. D. C.; Mullen, K.; Bredas, J. L. *Chem. Phys. Lett.* **1997**, *278* (1–3), 139–145.
 (32) Sluch, M. I.; Godt, A.; Bunz, U. H. F.; Berg, M. A. *J. Am. Chem. Soc.* **2001**, *123* (26), 6447–6448.
 (33) Karabunarliev, S.; Baumgarten, M.; Bittner, E. R.; Mullen, K. *J. Chem. Phys.* **2000**, *113* (24), 11372–11381.
 (34) Gierschner, J.; Mack, H.-G.; Luer, L.; Oelkrug, D. *J. Chem. Phys.* **2002**, *116* (19), 8596–8609.
 (35) Heimel, G.; Daghofer, M.; Gierschner, J.; List, E. J. W.; Grimsdale, A. C.; Mullen, K.; Beljonne, D.; Bredas, J.-L.; Zojler, E. *J. Chem. Phys.* **2005**, *122* (5), 054501–11.
 (36) Liu, L. T.; Yaron, D.; Sluch, M. I.; Berg, M. A. *J. Phys. Chem. B* **2006**, *110* (38), 18844–18852.
 (37) Keil, T. H. *Phys. Rev.* **1965**, *140* (2A), A601–A601.
 (38) Myers, A. B.; Trulson, M. O.; Mathies, R. A. *J. Chem. Phys.* **1985**, *83* (10), 5000–5006.
 (39) Fiesel, R.; Halkyard, C. E.; Rampey, M. E.; Kloppenburg, L.; Studer-Martinez, S. L.; Scherf, U.; Bunz, U. H. F. *Macromol. Rapid Commun.* **1999**, *20* (3), 107–111.
 (40) Kim, J.; Swager, T. M. *Nature (London)* **2001**, *411* (6841), 1030–1034.
 (41) Okuyama, K.; Hasegawa, T.; Ito, M.; Mikami, N. *J. Phys. Chem.* **1984**, *88* (9), 1711–1716.
 (42) Crisp, G. T.; Bubner, T. P. *Tetrahedron* **1997**, *53* (34), 11899–11912.
 (43) Crisp, G. T.; Bubner, T. P. *Tetrahedron* **1997**, *53* (34), 11881–11898.
 (44) McFarland, S. A.; Finney, N. S. *J. Am. Chem. Soc.* **2002**, *124* (7), 1178–1179.
 (45) Hu, W.; Zhu, N.; Tang, W.; Zhao, D. *Org. Lett.* **2008**, *10* (13), 2669–2672.

(46) Brizius, G.; Billingsley, K.; Smith, M. D.; Bunz, U. H. F. *Org. Lett.* **2003**, *5* (21), 3951–3954.

(47) Yang, J. S.; Yan, J. L.; Hwang, C. Y.; Chiou, S. Y.; Liao, K. L.; GavinTsai, H. H.; Lee, G. H.; Peng, S. M. *J. Am. Chem. Soc.* **2006**, *128* (43), 14109–14119.

(48) Otsuda, K.; Kitagawa, Y.; Kimura, S.; Imanishi, Y. *Biopolymers* **1993**, *33* (9), 1337–1345.

(49) Chen, Y.-H.; Yang, J. T.; Martinez, H. M. *Biochemistry* **1972**, *11* (22), 4120–4131.

(50) Vijayakumar, E. K. S.; Balam, P. *Tetrahedron* **1983**, *39* (16), 2725–2731.

(51) Holzwarth, G.; Doty, P. *J. Am. Chem. Soc.* **1965**, *87* (2), 218–228.

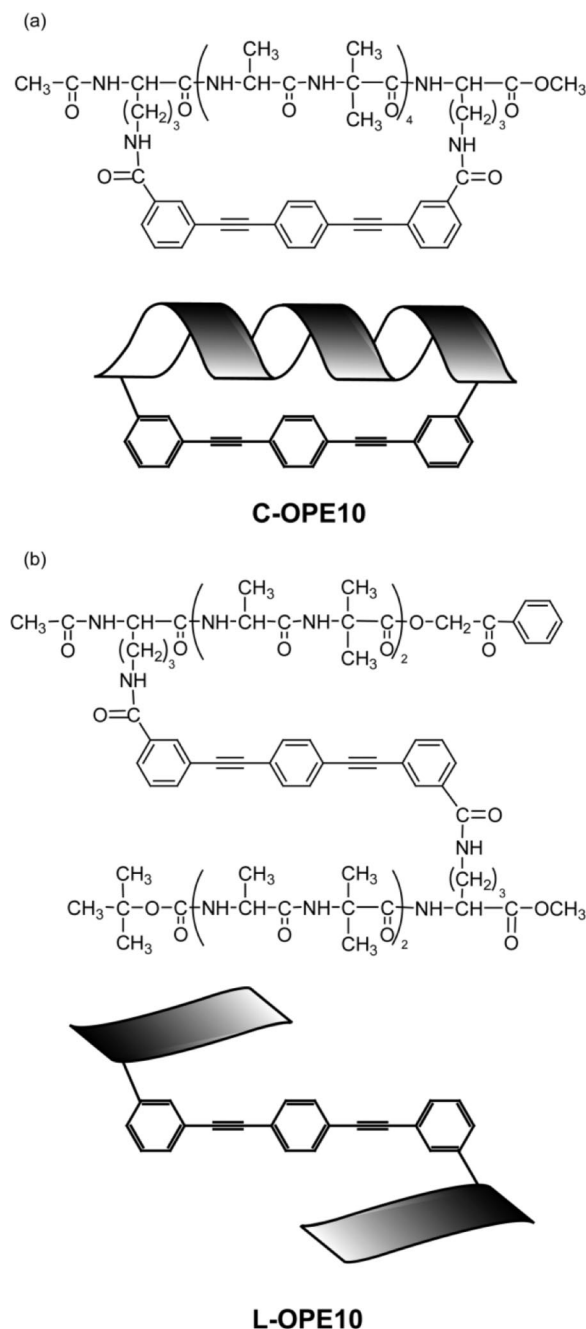


FIGURE 1. Chemical structures and schematic presentations of (a) **C-OPE10** and (b) **L-OPE10**.

indicate that the α -helical structure is most dominant in the decamer but has only a little advantage in stabilization against other structures.^{52–55} Because the molar ellipticity per residue of the **C-OPE10** (ca. -1×10^4 deg cm² dmol⁻¹ residue⁻¹ at 222 nm) was close to that of the free dodecamer of five repeats of the Ala-Aib alternating sequence,⁵² the decapeptide moiety was not stabilized in its helical structure despite the connection

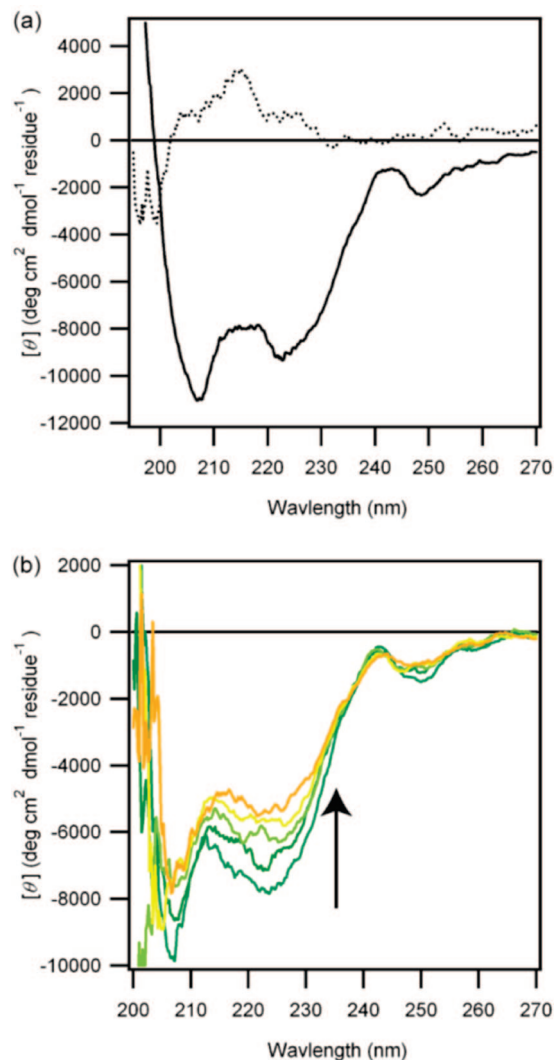


FIGURE 2. Circular dichroism (CD) spectra of (a) **C-OPE10** (solid) and **L-OPE10** (dot), and (b) temperature dependence of CD spectra of **C-OPE10** with raising from 10 (blue) to 50 °C (orange; every 10 °C).

of a rigid rod-shaped OPE like a molecular splint. One reason for failure in stabilization of the helical structure should be unsuitable geometry for the OPE moiety to bridge the two points of the peptide with taking α -helical structure. The distance between the two terminal residues of the α -helical decapeptide may be longer than the OPE counterpart, because the side chains of the two terminal residues make a dihedral angle of about 80° around the helix axis and are not straight along the helix axis. Another reason for instability in the α -helix may be competition between 3_{10} - and α -helical structures. When the temperature was raised to 50 °C, the peak at 222 nm nearly disappeared and became a shoulder, which is close to the typical CD spectrum pattern for 3_{10} -helical structure.⁵⁶

Characterization of the OPE Moiety. Absorption and emission spectra of **C-OPE10** and **L-OPE10** in methanol were measured (Figure 3). The absorption spectra of **C-OPE10** and **L-OPE10** showed well-resolved vibrational bands at 373, 340, and 320 nm, which is typical for OPE with a few functional

(52) Miura, Y.; Kimura, S.; Imanishi, Y.; Umemura, J. *Langmuir* **1998**, *14* (24), 6935–6940.

(53) Morita, T.; Kimura, S.; Kobayashi, S.; Imanishi, Y. *J. Am. Chem. Soc.* **2000**, *122* (12), 2850–2859.

(54) Kitagawa, K.; Morita, T.; Kimura, S. *J. Phys. Chem. B* **2004**, *108* (39), 15090–15095.

(55) Kai, M.; Takeda, K.; Morita, T.; Kimura, S. *J. Pept. Sci.* **2008**, *14* (2), 192–202.

(56) Toniolo, C.; Polese, A.; Formaggio, F.; Crisma, M.; Kamphuis, J. *J. Am. Chem. Soc.* **1996**, *118* (11), 2744–2745.

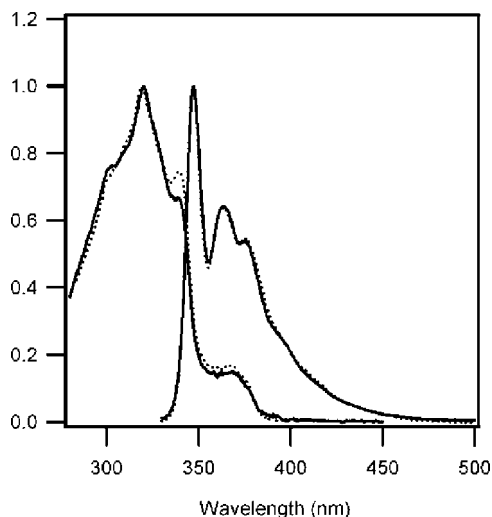


FIGURE 3. Normalized absorption and emission spectra of **C-OPE10** (solid) and **L-OPE10** (dot) in methanol.

groups.^{36,57,58} No sharp band at the longer wavelength was observed in both absorption spectra under the present conditions (ca. 15 μM for both **C-OPE10** and **L-OPE10**). The emission spectra of the both compounds also showed clear vibrational bands as the absorption spectra. The mirror image symmetry between absorption and emission spectra was broken similarly to the other reports on PPE/OPEs^{32,57} as well as poly(phenylenevinylene)s (PPVs)^{19,31,34} and poly(*p*-phenylene)s (PPPs).³⁵ When the two absorption spectra were normalized by the intensity at 320 nm, **C-OPE10** shows nearly identical absorption and emission spectra with **L-OPE10**. There are two possible interpretations for the identical spectra: one is the helix bridge does not hinder the free rotation of the aromatic groups around the ethynylene axis, and the other is the fixed conformation of the OPE moiety by the helix bridge happens to show similar spectra to the average conformation of the OPE moiety in **L-OPE10**, where nearly frictionless rotation is allowed around the ethynylene axis.^{18,41} We conclude the latter interpretation is applied to the present case as following.

To investigate the conformation of the OPE moiety, CD spectra were recorded in the absorption region of the OPE (260–360 nm). A negative Cotton effect was observed with **C-OPE10** (Figure 4), whereas no peaks with **L-OPE10**. CD spectra of π -conjugate polymers such as PPE,⁵⁹ PPV,⁶⁰ and PPP^{61,62} have been examined for the purpose of fabrication of circularly polarized electroluminescence materials. Cotton effects of those compounds appeared upon formation of chiral aggregation due to the chirality introduced in aliphatic side chains. This chiral aggregation is, however, not the case for **C-OPE10**, because no aggregation band in the absorption spectrum was observed in the present concentration range (13–16 μM). Both

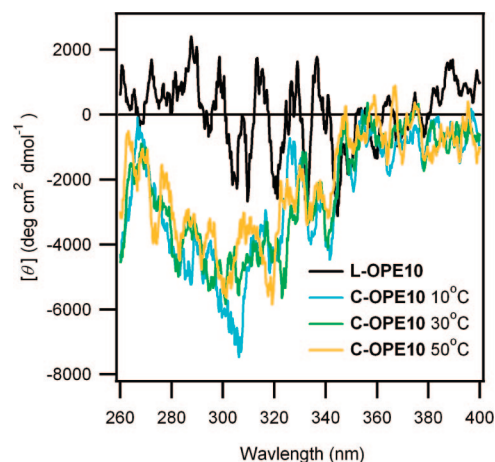


FIGURE 4. CD spectra of **C-OPE10** and **L-OPE10** in methanol.

C-OPE10 and **L-OPE10** were homogeneously dissolved in methanol. Therefore, the negative induced CD of **C-OPE10** should reflect a twist conformation of the OPE moiety upon bridging by a right-handed helix. As far as we know, this is the first example to prepare a π -conjugated compound having main-chain chirality by bridging the twisted OPE terminals with a chiral helix, which is distinctly different from the previous report by Fiesel et al. who have also synthesized soluble PPPs having main-chain chirality.⁶³

The negative Cotton effect of **C-OPE10** shows little change with increasing temperature, which is a sharp contrast to the peptide moiety. The reason may be due to the flexible linker between the OPE moiety and the helical peptide to buffer the influence of the thermal fluctuation of the helical peptide on the OPE moiety, but the detail remains to be solved.

The conformation of the OPE moiety is further studied by *ab initio* calculations on model compounds. To start with, geometry **1** (Figure 5) was prepared by optimization with the DFT method on the B3LYP/6-31G(d,p) level. The vibration analysis revealed that **1** located at a local minimum in the energy potential. The dihedral angles of the three phenyl rings of **1** were less than 1°. Geometries **2**, **R15**, and **L15** (Figure 5) were prepared by changing the dihedral angles between the phenyl rings from **1**. Geometry **2** is a coplanar conformation, where two substituents of the OPE moiety were located at the same side. Geometry **R15** has a dihedral angle of 15° between two adjacent phenyl rings in a right-handed way, whereas **L15** in a left-handed way. Single-point calculation on the four geometries were performed using TD-DFT method using B3LYP/6-31G(d,p) basis set. The predicted absorption and CD spectra are shown in Figure 6. The maximum absorption wavelength is 364 nm for **1** and **2**, and 361 nm for **R15** and **L15**. This reflects that the π -conjugation is weakened in **R15** and **L15** because the coplanar geometry of **2** is twisted. The calculated CD spectra of **R15** and **L15** show a negative and positive Cotton effect at the maximum absorbance wavelength, respectively (Figure 6b). It is thus concluded that the OPE moiety in **C-OPE10** should take the right-handed conformation. However, the calculated ellipticity of **R15** ($-3.3 \times 10^4 \text{ deg cm}^2 \text{ dmol}^{-1}$) is five times larger than the measured value (ca. $-6 \times 10^3 \text{ deg cm}^2 \text{ dmol}^{-1}$). CD spectra of **2** were calculated with varying the dihedral angles from 5 to 90° (Figure 7). The Cotton effect at

(57) Levitus, M.; Schmieder, K.; Ricks, H.; Shimizu, K. D.; Bunz, U. H. F.; Garcia-Garibay, M. A. *J. Am. Chem. Soc.* **2001**, *123* (18), 4259–4265.

(58) James, P. V.; Sudeep, P. K.; Suresh, C. H.; Thomas, K. G. *J. Phys. Chem. A* **2006**, *110* (13), 4329–4337.

(59) Fiesel, R.; Halkyard, C. E.; Rampey, M. E.; Kloppenburg, L.; Studer-Martinez, S. L.; Scherf, U.; Bunz, U. H. F. *Macromol. Rapid Commun.* **1999**, *20* (3), 107–111.

(60) Peeters, E.; Christiaans, M. P. T.; Janssen, R. A. J.; Schoo, H. F. M.; Dekkers, H. P. J. M.; Meijer, E. W. *J. Am. Chem. Soc.* **1997**, *119* (41), 9909–9910.

(61) Oda, M.; Nothofer, H. G.; Lieser, G.; Scherf, U.; Meskers, S. C. J.; Neher, D. *Adv. Mater.* **2000**, *12* (5), 362–365.

(62) Fiesel, R.; Scherf, U. *Acta Polym.* **1998**, *49* (8), 445–449.

(63) Fiesel, R.; Huber, J.; Apel, U.; Enkelmann, V.; Hentschke, R.; Scherf, U.; Cabrera, K. *Macromol. Chem. Phys.* **1997**, *198* (9), 2623–2650.

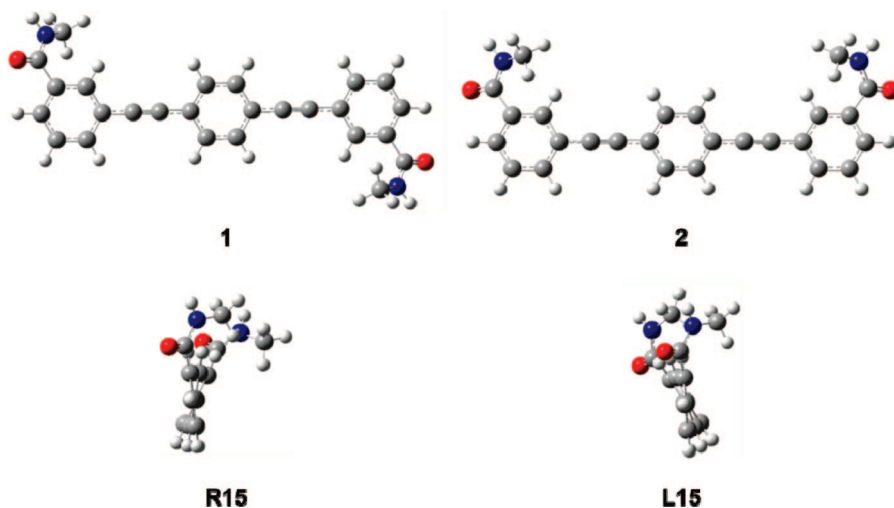


FIGURE 5. Geometries of the model compounds. A gray ball represents a carbon atom, white represents hydrogen, red represents oxygen, and blue represents nitrogen.

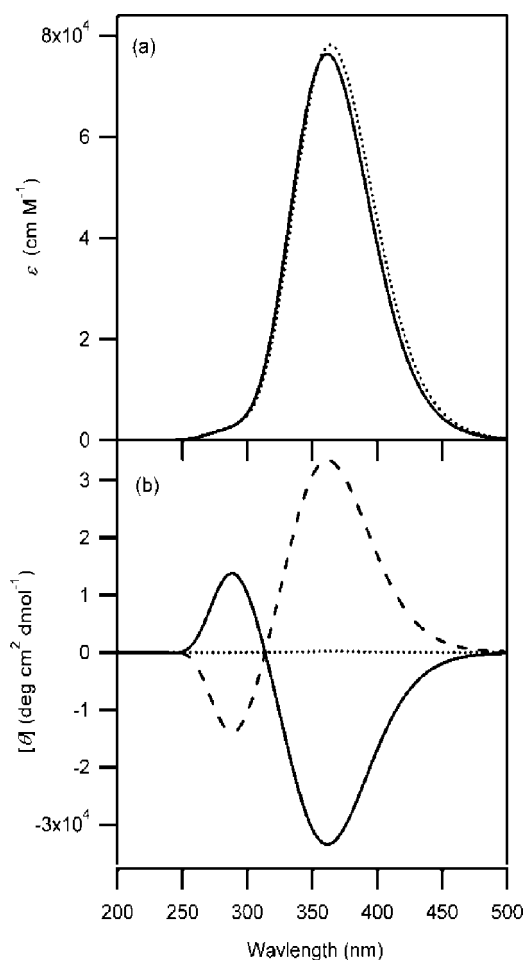


FIGURE 6. Computed (a) absorption and (b) CD spectra of geometries **1** (dot), **R15** (solid), and **L15** (dash). The absorption and CD spectra of **2** are nearly identical to those of **1**. The absorption spectra of **R15** and **L15** are also identical.

the maximum absorption wavelength increases as the twisting angle increases from 0 to 60°. If the twist angle is more than 60°, the negative Cotton effect starts decreasing sharply and finally drops down to zero at 90°, where chirality disappears. When the measured molar ellipticity is compared with the computed ones, the twisted angle is estimated to be less than

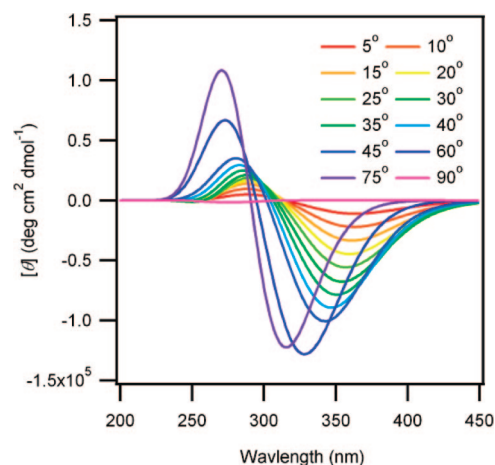


FIGURE 7. Calculated CD spectra on right-hand twisted geometries with varying the dihedral angles between two phenyl rings around the molecular axis.

5°. This estimation, however, is not reliable due to the imprecision of the calculated intensity. At the moment, the twisted angle is considered to be less than 15°.

Conclusions

Novel helical peptide-OPE conjugates **C-OPE10** (cyclized) and **L-OPE10** (linear) were prepared. From CD measurements, the decapeptide moiety in **C-OPE10** was revealed to take α -helical structure, whereas two pentamers in **L-OPE10** took random structure. Observation of the induced negative Cotton effect of the OPE moiety in **C-OPE10** indicated a twisted conformation of the OPE moiety in **C-OPE10** because two phenyl rings were bridged by the α -helical decapeptide. Calculations showed a right-handed twist conformation of the OPE moiety. We provide here a new method to prepare a π -conjugated compound having main-chain chirality by bridging the OPE with a chiral helix. Such compounds will be applied for interesting chiroptical materials. Further modification of OPE with another helical peptide to load more tension on the OPE moiety is now under investigation.

Experimental Section

Materials. **C-OPE10** and **L-OPE10** were synthesized according to Scheme S1 in Supporting Information. The peptides were

synthesized by the conventional liquid-phase method. The OPEs were synthesized by the Sonogashira coupling. Tetrahydrofuran (THF) used as solvent in the Sonogashira coupling was distilled over calcium hydride and butylated hydroxyl toluene. The other reagents were used as purchased. All intermediates were identified by ^1H NMR spectroscopy and some of them were further confirmed by fast atom bombardment (FAB) mass spectrometry. The NMR peak assignments for compounds **1–8** were confirmed with HH-COSY. The purity of the products was checked by thin layer chromatography (TLC). The purity of the final compounds were further analyzed by HPLC (ODS column, eluant: $\text{CH}_3\text{CN}/\text{H}_2\text{O}$ /trifluoroacetic acid = 45/55/0.05 for **C-OPE10**; $\text{CH}_3\text{CN}/\text{H}_2\text{O}$ = 90/10 for **L-OPE10**; flow rate: 1 mL/min; monitor at 355 nm).

Synthesis. Boc-(Ala-Aib) $_2$ -OPac (2). To Boc-(Ala-Aib) $_2$ -OH (550 mg, 1.29 mmol) in DMF were added phenacylbromide (513 mg, 2.58 mmol) and triethylamine (TEA; 360 μL , 2.58 mmol) at 0 $^\circ\text{C}$. The reaction mixture was stirred at room temperature for 3 h, followed by concentration under reduced pressure. The residue was taken up with chloroform and washed with 4% aq NaHCO_3 (3 \times), brine, 4% aq KHSO_4 (2 \times), and brine. The organic layer was dried over MgSO_4 and concentrated under reduced pressure. The residue was washed with hexane and diisopropylether, giving 677 mg (1.23 mmol, 95% yield).

^1H NMR (400 MHz, CDCl_3) δ 1.35–1.39 (m, 6H, AlaC $^\beta$), 1.42 (s, 9H, Boc), 1.57 (s, 3H, AibC $^\beta$), 1.61 (s, 3H, AibC $^\beta$), 1.64 (s, 3H, AibC $^\beta$), 1.70 (s, 3H, AibC $^\beta$), 3.95 (m, 1H, AlaC $^\alpha$), 4.47 (m, 1H, AlaC $^\alpha$), 4.99 (s, 1H, urethane), 5.33 (s, 2H, OCH_2COPh), 6.56 (s, 1H, NHCO), 7.32 (s, 1H, NHCO), 7.33 (s, 1H, NHCO), 7.49 (t, 2H, aromatic), 7.62 (d, 1H, aromatic), 7.92 (d, 2H, aromatic). FAB-MS (matrix: 3-nitrobenzylalcohol (NBA)) calcd for $\text{C}_{27}\text{H}_{41}\text{N}_4\text{O}_8$ [(M + H) $^+$], 549.28; found, 549.4.

Boc-Orn(Z)-(Ala-Aib) $_2$ -OPac (3). Compound **2** (676 mg, 1.23 mmol) was treated with 4 N HCl/dioxane. The HCl salt was washed with diethylether. To the peptide in DMF were added Boc-Orn(Z) (667 mg, 1.82 mmol), *O*-(7-azabenzotriazol-1-yl)-1,1,3,3-tetramethyluronium hexafluorophosphate (HATU; 923 mg, 2.43 mmol), and diisopropylethylamine (DIEA; 739 μL , 4.25 mmol) at 0 $^\circ\text{C}$. The reaction mixture was stirred under a N_2 atmosphere at room temperature for 30 h. Additional portions of HATU (200 mg, 0.53 mmol) and DIEA (120 μL , 0.70 mmol) were added to the mixture at 0 $^\circ\text{C}$. The mixture was further stirred for 10 h and concentrated under reduced pressure. The residue was taken up with ethyl acetate and washed with water, 4% aq NaHCO_3 (3 \times), brine, 4% aq KHSO_4 (2 \times), and brine. The organic layer was dried over MgSO_4 and concentrated under reduced pressure. The residue was further purified with column chromatography (silica gel, chloroform/methanol = 50/1), giving 830 mg (1.03 mmol, 85% yield).

^1H NMR (400 MHz, CDCl_3) δ 1.37–1.60 (m, 29H, AibC $^\beta$, AlaC $^\beta$, OrnC $^\beta$, Boc), 1.75 (m, 2H, OrnC $^\gamma$), 3.24–3.17 (m, 2H, OrnC $^\delta$), 4.02 (s, 1H, OrnC $^\alpha$), 4.02 (s, 1H, OrnC $^\alpha$), 4.11 (m, 1H, AlaC $^\alpha$), 4.41 (m, 1H, AlaC $^\alpha$), 5.07 (s, 2H, COOCH_2Ph), 5.12 (s, 1H, OrnNH $^\delta$), 5.33 (s, 2H, OCH_2COPh), 5.42 (s, 1H, OrnNH $^\alpha$), 6.72 (s, 1H, AlaNH), 7.06 (d, 1H, AlaNH), 7.16 (s, 1H, AibNH), 7.29–7.36 (m, 6H, aromatic and AibNH), 7.49 (t, 2H, aromatic), 7.62 (m, 1H, aromatic), 7.92 (d, 2H, aromatic). FAB-MS (matrix: NBA) Calcd for $\text{C}_{40}\text{H}_{57}\text{N}_6\text{O}_{11}$ [(M + H) $^+$], 797.40; found, 797.3.

Ac-Orn(Z)-(Ala-Aib) $_2$ -OPac (4). Compound **3** (830 mg, 1.04 mmol) was treated with 4 N HCl/dioxane. The HCl salt was washed with diethylether. To the peptide were added acetic anhydride (3 mL) and pyridine (9 mL). The reaction mixture was stirred at room temperature for 30 h, and the solution was poured into water. The aqueous layer was extracted with chloroform. The organic layer was washed with brine, dried over MgSO_4 , and concentrated under reduced pressure. The residue was purified with column chromatography (silica gel, chloroform/methanol = 50/1, then 10/1), giving 630 mg (0.85 mmol, 88%).

^1H NMR (400 MHz, CDCl_3) δ 1.37–1.60 (m, 20H, AibC $^\beta$, AlaC $^\beta$, OrnC $^\beta$), 1.81 (m, 2H, OrnC $^\gamma$), 2.03 (s, 3H, Ac), 3.17–3.24 (m, 2H, OrnC $^\delta$), 4.02 (s, 1H, OrnC $^\alpha$), 4.11 (m, 1H, AlaC $^\alpha$), 4.41

(m, 1H, AlaC $^\alpha$), 5.07 (dd, 2H, COOCH_2Ph), 5.12 (s, 1H, OrnNH $^\delta$), 5.33 (dd, 2H, OCH_2COPh), 6.80 (s, 1H, OrnNH $^\alpha$), 6.93 (d, 1H, AlaNH), 7.06–7.13 (m, 2H, AibNH), 7.29–7.36 (m, 6H, aromatic and AibNH), 7.49 (t, 2H, aromatic), 7.62 (m, 1H, aromatic), 7.92 (d, 2H, aromatic).

Ac-Orn(Phl)-(Ala-Aib) $_2$ -OPac (5). Compound **4** (630 mg, 0.852 mmol) was treated with HBr/AcOH. The HBr salt was washed with diethylether. To the peptide in DMF were added 3-iodobenzoic acid (434 mg, 1.75 mmol), HATU (1.33 g, 3.5 mmol), and DIEA (914 μL , 5.25 mmol) at 0 $^\circ\text{C}$, and the mixture was kept stirring under a N_2 atmosphere at room temperature for 30 h. The mixture was concentrated under reduced pressure. The residue was taken up with chloroform and washed with water, 4% aq NaHCO_3 (3 \times), brine, 4% aq KHSO_4 (2 \times), and brine. The organic layer was dried over MgSO_4 and concentrated under reduced pressure. The residue was further purified with a column chromatography (silica gel, chloroform/methanol = 30/1) and washed with diisopropylether, giving 448 mg (0.537 mmol, 61% yield).

^1H NMR (400 MHz, CDCl_3) δ 1.37–1.60 (m, 20H, AibC $^\beta$, AlaC $^\beta$, OrnC $^\beta$), 1.81 (m, 2H, OrnC $^\gamma$), 2.06 (s, 3H, Ac), 3.51 (m, 2H, OrnC $^\delta$), 4.07 (m, 1H, AlaC $^\alpha$), 4.35 (m, 1H, AlaC $^\alpha$), 4.44 (m, 1H, OrnC $^\alpha$), 5.30 (dd, 2H, OCH_2COPh), 6.78–6.83 (m, 2H, OrnNH $^\delta$, AibNH), 7.07–7.13 (m, 2H, AlaNH, OrnNH $^\alpha$), 7.15–7.21 (m, 2H, AlaNH, aromatic), 7.32 (s, 1H, AibNH), 7.50 (m, 2H, aromatic), 7.62 (m, 1H, aromatic), 7.85 (d, 1H, aromatic), 7.85–7.96 (m, 3H, aromatic), 8.18 (s, 1H, aromatic). FAB-MS (matrix: NBA) Calcd for $\text{C}_{36}\text{H}_{48}\text{IN}_6\text{O}_9$ [(M + H) $^+$], 835.24; found, 835.3.

Boc-(Ala-Aib) $_2$ -Orn(Z)-OMe (6). To **1** (1.36 g, 3.16 mmol) and the HCl salt of Orn(Z)-OMe (1.20 g, 3.79 mmol) in DMF were added HATU (1.80 g, 4.74 mmol) and DIEA (1.93 mL, 11.1 mmol) at 0 $^\circ\text{C}$. The reaction mixture was kept stirring under a N_2 atmosphere for 22 h. The mixture was concentrated under reduced pressure. The residue was taken up with ethyl acetate and washed with water, 4% aq NaHCO_3 (3 \times), brine, 4% aq KHSO_4 (2 \times), and brine. The organic layer was dried over MgSO_4 and concentrated under reduced pressure. The product was further purified with a column chromatography (silica gel, chloroform/methanol = 50/1), giving 1.36 g (1.96 mmol, 62%).

^1H NMR (400 MHz, CDCl_3) δ 1.37–1.64 (m, 27H, AibC $^\beta$, Boc, AlaC $^\beta$), 1.76–1.90 (m, 4H, OrnC $^\beta$, OrnC $^\gamma$), 3.21 (s, 2H, OrnC $^\delta$), 3.68 (s, 3H, OCH_3), 3.88 (m, 1H, AlaC $^\alpha$), 4.05 (m, 1H, AlaC $^\alpha$), 4.44 (m, 1H, OrnC $^\alpha$), 5.05 (s, 2H, COOCH_2Ph), 5.20 (s, 1H, AlaNH), 5.67 (s, 1H, OrnNH $^\delta$), 6.49 (s, 1H, AibNH), 7.28 (s, 1H, OrnNH $^\alpha$), 7.31 (s, 5H, aromatic), 7.62 (d, 1H, AlaNH). FAB-MS (matrix: NBA) Calcd for $\text{C}_{33}\text{H}_{53}\text{N}_6\text{O}_{10}$ [(M + H) $^+$], 693.37; found, 693.4.

Boc-(Ala-Aib) $_2$ -Orn(Phl)-OMe (7). To **6** (1.3 g, 1.88 mmol) in methanol was added Pd/C (260 mg). The reaction mixture was kept stirring under a H_2 atmosphere for 24 h. Another portion of Pd/C (50 mg) was added to the mixture and stirred for another 26 h. The catalyst was filtered off, and the filtrate was concentrated under reduced pressure. To the peptide in DMF were added 3-iodobenzoic acid (592 mg, 2.39 mmol), HATU (1.51 g, 3.98 mmol), and DIEA (0.832 μL , 4.78 mmol) at 0 $^\circ\text{C}$. The reaction mixture was kept stirring under a N_2 atmosphere for 14 h at room temperature. Additional portions of HATU (600 mg, 1.6 mmol) and DIEA (554 μL , 3.2 mmol) were added to the mixture and stirred for 24 h. The mixture was concentrated under reduced pressure. The residue was taken up with chloroform and washed with water, 4% aq NaHCO_3 (3 \times), brine, 4% aq KHSO_4 (2 \times), and brine. The organic layer was dried over MgSO_4 and concentrated under reduced pressure. The residue was further purified by a column chromatography (silica gel, chloroform/methanol = 50/1, then 10/1), giving 451 mg (0.80 mmol, 35%).

^1H NMR (400 MHz, CDCl_3) δ 1.37–1.68 (m, 27H, AibC $^\beta$, Boc, AlaC $^\beta$), 1.72 (m, 2H, OrnC $^\gamma$), 1.98 (m, 2H, OrnC $^\beta$), 3.37 (m, 2H, OrnC $^\delta$), 3.69 (s, 3H, OCH_3), 3.93 (m, 1H, AlaC $^\alpha$), 4.21 (m, 1H, AlaC $^\alpha$), 4.50 (m, 1H, OrnC $^\alpha$), 6.42 (s, 1H, AlaNH), 7.12 (m, 1H, aromatic), 7.31 (m, 1H, OrnNH $^\alpha$), 7.35 (s, 1H, AibNH), 7.54 (S,

1H, OrnNH^δ), 7.60 (d, 1H, AlaNH), 7.76 (d, 1H, aromatic), 7.92 (d, 1H, aromatic), 8.22 (s, 1H, aromatic). FAB-MS (matrix: NBA) Calcd for C₃₂H₅₀N₆O₉ [(M + H)⁺], 789.26; found, 789.3.

Boc-(Ala-Aib)₂-Orn(DPE)-OMe (8). To **7** (308 mg, 390 μmol) and 1,4-diethynylbenzene (59 mg, 468 μmol) in THF were added Pd(PPh₃)₂Cl₂ (16.5 mg, 23.4 μmol), CuI (7.4 mg, 39 μmol), and DIEA (272 μL, 1.56 mmol) at 0 °C. The reaction mixture was kept stirring under an Ar atmosphere for 2 h. The mixture was then concentrated under reduced pressure. The residue was purified by a column chromatography (silica gel, chloroform/methanol = 30/1), giving 130 mg (165 μmol, 42%).

¹H NMR (400 MHz, CDCl₃) δ 1.35–1.57 (m, 27H, AibC^β, Boc, AlaC^β), 1.75 (m, 2H, OrnC^γ), 2.00 (m, 2H, OrnC^β), 3.17 (s, 1H, HCCPh), 3.48 (m, 2H, OrnC^δ), 3.71 (s, 3H, OCH₃), 3.92 (m, 1H, AlaC^α), 4.17 (m, 1H, AlaC^α), 4.52 (m, OrnC^α), 4.99 (s, 1H, AlaNH), 6.40 (s, 1H, AibNH), 7.01 (s, 1H, AibNH), 7.31–7.40 (m, 2H, OrnNH^α, aromatic), 7.42–7.51 (m, 5H, AlaNH, aromatic), 7.58 (d, 1H, aromatic), 7.88 (d, 1H, aromatic), 8.18 (s, 1H, aromatic). FAB-MS (matrix: NBA) Calcd for C₄₂H₅₅N₆O₉ [(M + H)⁺], 787.40; found, 787.4.

L-OPE10. To **8** (110 mg, 140 μmol) and **5** (140 mg, 167 μmol) in THF were added Pd(PPh₃)₂Cl₂ (5.9 mg, 8.4 μmol), CuI (2.7 mg, 14 μmol), and DIEA (97 μL, 560 μmol) at 0 °C. The reaction mixture was kept stirring under an Ar atmosphere for 3 h. The reaction mixture was concentrated under reduced pressure. The residue was purified by a Sephadex LH20 column (eluant: DMF), giving 106 mg (67.2 μmol, 48% at most). HPLC: retention time = 6.377 min (93%).

¹H NMR (400 MHz, CDCl₃) δ 1.35–1.59 (m, 45H, AibC^β, Boc, AlaC^β), 1.59–1.90 (m, 8H, OrnC^β, OrnC^γ), 2.07 (s, 3H, Ac), 3.40–3.55 (m, 4H, OrnC^δ), 3.71 (s, 3H, OCH₃), 3.92 (m, 1H, AlaC^α, or OrnC^α), 4.06 (m, 1H, AlaC^α, or OrnC^α), 4.14 (m, 1H, AlaC^α, or OrnC^α), 4.36 (m, 1H, AlaC^α, or OrnC^α), 4.42 (m, 1H, AlaC^α, or OrnC^α), 4.51 (m, 1H, AlaC^α, or OrnC^α), 5.20 (s, 1H, AlaC^α, or OrnC^α), 5.30 (dd, 2H, OCH₂COPh), 6.53 (s, 1H, NH), 6.88 (s, 1H, NH), 7.00 (d, 1H, NH), 7.35–7.95 (m, 21H, NH, and aromatic). FAB-MS (matrix: NBA) Calcd for C₇₈H₁₀₁N₁₂O₁₈ [(M + H)⁺], 1493.73; found, 1493.9.

C-OPE10. L-OPE10 (74 mg, 49 μmol) in methanol (200 μL) and 1,4-dioxane (200 μL) was treated with 1 N NaOH (60 μL) at 0 °C without stirring for 4 h. The mixture was neutralized with HCl aq and concentrated under reduced pressure. The product was treated with trifluoroacetic acid (730 μL) in the presence of anisole (73 μL) at 0 °C for 1 h. The mixture was concentrated under reduced pressure, and the residue was washed with diethyl ether. The identification was carried out by FAB-MS. To the trifluoroacetic acid salt of the peptide in DMF were added HATU (205 mg, 539 μmol) and 1-hydroxy-7-azabenzotriazole (HOAt; 73 mg, 539 μmol). The mixture was kept stirring under a N₂ atmosphere at 0 °C. To the solution was added a DMF solution of DIEA (0.1 M, 10.8 mL) over 1.5 h. The temperature was then gradually raised to room temperature and the mixture was stirred for 24 h. Additional portions of HATU (41 mg, 108 μmol), HOAt (14.7 mg, 108 μmol), and DIEA (28 μL, 162 μmol) were added to the mixture at 0 °C followed by 33 h of stirring at room temperature. The mixture was concentrated under reduced pressure and purified by a Sephadex LH-20 column for two times (eluent: DMF and methanol) and preparative TLC (eluent: chloroform/methanol 10/1). Finally, the product was solidified with hexane, giving 10 mg (7.6 μmol, 14% at most). HPLC: retention time = 4.713 min (~100%).

¹H NMR (400 MHz, MeOH-*d*₄) δ 1.35–1.57 (m, 36H, AibC^α, AlaC^α), 1.75–1.98 (m, 8H, OrnC^β, OrnC^γ), 2.04 (s, 3H, Ac), 3.48

(m, 4H, OrnC^δ), 3.69 (s, 3H, OCH₃), 3.92–4.04 (m, 3H, AlaC^α, or OrnC^α), 4.13–4.17 (m, 1H, AlaC^α, or OrnC^α), 4.29 (m, 1H, AlaC^α, or OrnC^α), 7.49–8.10 (m, 12H, aromatic). FAB-MS (matrix: NBA) Calcd for C₆₅H₈₅N₁₂O₁₄ [(M + H)⁺], 1257.62; found, 1257.7.

Spectroscopy in Solution. CD spectra were measured by a spectropolarimeter. Optical cells of a 0.1 and 1 cm optical path length were used. The accumulation number was four. The helix contents of the peptides were calculated from eq 1.⁴⁹

$$f_H(\%) = -([\theta]_{222} + 2340)/30300 \quad (1)$$

f_H and $[\theta]_{222}$ represent the helix content and molar ellipticity in residue concentration at 222 nm, respectively. An optical cell of a 1 cm optical path length was used in both absorption and emission spectroscopic measurements.

Quantum Calculation. *ab initio* Calculations were carried out on a Gaussian, Inc. Gaussian 03 program⁶⁴ using the density functional theory (DFT) with the Becke's three parameter hybrid functional and Lee–Yang–Parr correlation (B3LYP) method⁶⁵ with the 6-31G(d,p)⁶⁶ basis set. The optimized geometry was initially generated on a Semicem, Inc. Gaussview program,⁶⁷ then optimized by the DFT method on Gaussian 03. The optimized geometry was checked by the frequency analysis. It was confirmed that no imaginary frequency number was outputted. The other geometries were generated from the optimized geometry by tuning the dihedral angle between two of the three phenyl rings. TD-DFT method^{68–70} was used for absorption and electric circular dichroism simulations.^{71,72} Ten singlet excited states were solved in the calculations.

Supporting Information Available: A synthetic scheme, proton and carbon NMR spectra of **L-OPE10** and **C-OPE10**, total energies and atom coordinates of **1**, **2**, **R30**, and **L30**. This material is available free of charge via the Internet at <http://pubs.acs.org>.

JO9001905

(64) Frisch, M. J.; Trucks, G. W.; Schlegel, H. B.; Scuseria, G. E.; Robb, M. A.; Cheeseman, J. R.; Montgomery, J. A.; Vreven, T.; Kudin, K. N.; Burant, J. C.; Millam, J. M.; Iyengar, S. S.; Tomasi, J.; Barone, V.; Mennucci, B.; Cossi, M.; Scalmani, G.; Rega, N.; Petersson, G. A.; Nakatsuji, H.; Hada, M.; Ehara, M.; Toyota, K.; Fukuda, R.; Hasegawa, J.; Ishida, M.; Nakajima, T.; Honda, Y.; Kitao, O.; Nakai, H.; Klene, M.; Li, X.; Knox, J. E.; Hratchian, H. P.; Cross, J. B.; Bakken, V.; Adamo, C.; Jaramillo, J.; Gomperts, R.; Stratmann, R. E.; Yazyev, O.; Austin, A. J.; Cammi, R.; Pomelli, C.; Ochterski, J. W.; Ayala, P. Y.; Morokuma, K.; Voth, G. A.; Salvador, P.; Dannenberg, J. J.; Zakrzewski, V. G.; Dapprich, S.; Daniels, A. D.; Strain, M. C.; Farkas, O.; Malick, D. K.; Rabuck, A. D.; Raghavachari, K.; Foresman, J. B.; Ortiz, J. V.; Cui, Q.; Baboul, A. G.; Clifford, S.; Cioslowski, J.; Stefanov, B. B.; Liu, G.; Liashenko, A.; Piskorz, P.; Komaromi, I.; Martin, R. L.; Fox, D. J.; Keith, T.; Al-Laham, M. A.; Peng, C. Y.; Nanayakkara, A.; Challacombe, M.; Gill, P. M. W.; Johnson, B.; Chen, W.; Wong, M. W.; Gonzalez, C.; and Pople, J. A. *Gaussian 03*, Revision E.01; Gaussian, Inc.: Wallingford, CT, 2004.

(65) Becke, A. D. *J. Chem. Phys.* **1993**, *98* (7), 5648–5652.

(66) Ditchfield, R.; Hehre, W. J.; Pople, J. A. *J. Chem. Phys.* **1971**, *54* (2), 724–728.

(67) Dennington, R., II; Keith, T.; Millam, J. *GaussView*, version 4.1; Semicem, Inc: Shawnee Mission, KS, 2007.

(68) Stratmann, R. E.; Scuseria, G. E.; Frisch, M. J. *J. Chem. Phys.* **1998**, *109* (19), 8218–8224.

(69) Bauernschmitt, R. d.; Ahlrichs, R. *Chem. Phys. Lett.* **1996**, *256* (4–5), 454–464.

(70) Casida, M. E.; Jamorski, C.; Casida, K. C.; Salahub, D. R. *J. Chem. Phys.* **1998**, *108* (11), 4439–4449.

(71) Bak, K. L.; Hansen, A. E.; Ruud, K.; Helgaker, T.; Olsen, J.; Jørgensen, P. *Theor. Chim. Acta* **1995**, *90* (5), 441–458.

(72) Autschbach, J.; Ziegler, T.; van Gisbergen, S. J. A.; Baerends, E. J. *J. Chem. Phys.* **2002**, *116* (16), 6930–6940.